

Exciton absorption properties of coherently coupled exciton-biexciton systems in quantum dots

Hideki Gotoh, Hidehiko Kamada, and Tadashi Saitoh*

NTT Basic Research Laboratories, NTT Corporation 3-1, Morinosato-Wakamiya, Atsugi-shi, Kanagawa 243-0198, Japan

Hiroaki Ando

Department of Physics, Konan University, 8-9-1 Okamoto Higashinadaku, Kobe 658-8501, Japan

Jiro Temmyo

Research Institute of Electronics, Shizuoka University, 3-5-1 Johoku, Hamamatsu, Shizuoka 422-8529, Japan

(Received 17 December 2004; published 31 May 2005)

Exciton-biexciton coherent coupling effects are examined in semiconductor quantum dots. The exciton absorption spectrum is measured with the microphotoluminescence excitation technique in a single InGaAs quantum dot. The spectrum changes from a Lorentzian-type line shape to an unusual dip-shaped line shape with increasing excitation intensities in a higher exciton state where there is a large oscillator strength between the exciton and biexciton states. The intensity dependence of the dip energy width clearly indicates that coherent Rabi oscillation occurs between the exciton and biexciton states. The absorption properties with excitation light of different polarizations show that the dip-shaped spectra only appear when there is a large biexciton state population with linear polarization. A theoretical analysis undertaken with the density matrix method agrees well with experimental results. This agreement reveals that exciton-biexciton coherent interactions lead to unusual absorption spectra and contribute crucially to the optical properties of quantum dots. The exciton-biexciton coherent effects provide a scheme for controlling four distinguishable states, which can be applied to a demonstration of quantum gate operations.

DOI: 10.1103/PhysRevB.71.195334

PACS number(s): 78.67.Hc, 71.35.-y, 42.50.Md, 78.55.Cr

I. INTRODUCTION

Semiconductor quantum dots have been the subject of many studies because of their intriguing physics and many novel device applications.^{1,2} Recently, semiconductor quantum dots have been attracting a lot of attention as a good candidate for the fundamental gates of the quantum computer, which is a new concept of quantum information processes.³⁻⁸ Excitons created by optical pulses become quantum bits (Q-bits), which are basic units of quantum gates, and sequences of optical pulses control gate operations. These quantum gates rely on two characteristics of excitons in quantum dots. One is the density-of-states in quantum dots and the other is the spatial size of quantum dot structures.

The density-of-states in a quantum dot is discrete and comb-shaped. In this density-of-states, most of the scattering processes for electrons and excitons are suppressed. This leads to long-lived exciton coherence, which is a notable characteristic of quantum dots and a key requirement as regards implementing Q-bit control processes. Experimental reports have confirmed that the exciton coherence time is much longer than that in quantum wells and bulk.⁹⁻¹¹ All quantum gate operations with quantum dots are based on exciton coherence. This long-lived coherence leads to many quantum gate operations, which will be indispensable in terms of implementing quantum computing.

Another characteristic is the nanoscale structure of quantum dots. When an exciton and a biexciton are confined in this small space, their binding energy is increased. The reported binding energy is about 20 meV for excitons and 5–10 meV for biexcitons,¹²⁻¹⁴ which is much larger than

those in bulk and quantum wells and results from three-dimensional confinement effects. Quantum dots provide an exciton-biexciton system that is very stable in the face of any thermal scattering event. This system has not yet been obtained in other semiconductor structures and may provide unprecedented optical physics. An exciton and a biexciton act as two Q-bits that interact with each other. Quantum gate operations using an exciton and a biexciton have already been proposed.¹⁵

In an exciton-biexciton system, biexciton-related coherent effects have a great influence on exciton coherence. Such a system exhibits coherence between an exciton and the ground states as well as between an exciton and a biexciton states. However, most studies have dealt only with the coherence of an exciton and discussions on decoherence processes have mainly been examined in terms of exciton-phonon interactions.⁹⁻¹¹ Since a biexciton is composed of two excitons, the coherence between an exciton and a biexciton may influence the exciton decoherence processes and also excitonic optical properties. The effects of biexcitons on exciton decoherence processes have been examined.¹⁶ The results indicate that coherent interactions between excitons and biexcitons contribute crucially to exciton decoherence processes.

The coherently coupled exciton-biexciton system can be regarded as a coherent three-level system. This three-level system is often studied in quantum atom optics.^{17,18} These studies have provided intriguing quantum interference effects such as coherent trapping and electromagnetically induced transparency (EIT), which provide novel optical device functions. Quantum dots may enable us to observe these effects with an exciton-biexciton coherent coupled system. More-

over, in an exciton-biexciton system, larger dipole moments than those in atoms are available due to the collective effect in many atoms and the mesoscopic enhancement effect in nanostructures.^{19,20} These may result in optical nonlinear effects with a small intensity light and also novel coherent phenomena that are applicable to future optical devices. A clarification of the physical properties of the exciton-biexciton system should provide us with important and valuable information on the physics of exciton coherence, the characteristics of quantum interference and possible quantum device applications.

In this paper, we investigate the optical properties of excitons in a coherently coupled exciton-biexciton system in quantum dots. We clarify the influence of the coherent effects between an exciton and a biexciton on the exciton photoabsorption properties in InGaAs quantum dots. Absorption spectra are measured in a single isolated quantum dot with the microphotoluminescence excitation (micro-PLE) technique. An exciton higher state and a biexciton higher state are coherently coupled by a single excitation laser. The coherent effects can be evaluated from the PL signals of an exciton and a biexciton. These coherent coupling effects depend on the biexciton population, the oscillator strength and the dipole moment between an exciton and a biexciton state. We measure the absorption spectra for different excitation intensities in two different exciton higher states whose dipole moments differ greatly. In the exciton state of the smaller dipole moment, Lorentzian-shaped absorption spectra are observed independent of excitation intensity. However, in the exciton state of the larger dipole moment, unusual exciton absorption spectra with a dip-shaped structure, in other words, energy splitting, are found at a high excitation intensity. The energy splitting increases in proportion to the square of the excitation intensity. This dependence is the same as that of Rabi splitting, which is a well-known coherent effect. Moreover, the energy splitting is found to depend strongly on the polarization of the excitation light, which is another proof of the existence of the coherent effects. We show that the coherent effects can be controlled by controlling the polarization of the excitation light. To confirm our experimental results, we numerically analyze the exciton-biexciton system with a simple density matrix method. We calculate exciton absorption spectra for different dipole moments and dephasing times, which characterize the coherent effects. The calculated results confirm that the unusual spectra are yielded by the strong coherent coupling effects between an exciton and a biexciton. The coherent coupling effects can be explained in terms of the dressed-atom picture, which is often used for strongly coupled atom-photon systems. This effect is also regarded as a quantum interference effect and is known as cascade type electromagnetically induced transparency (EIT).^{17,18} We discuss a possible scheme for accessing four distinguishable quantum states, which would be a good candidate for a quantum gate. Our results also provide information on exciton statistics, which are expected to yield novel exciton physics such as giant oscillator strength effects.

II. EXPERIMENT

The InGaAs quantum dot sample for our measurement was fabricated on a GaAs (311) B substrate by metalorganic

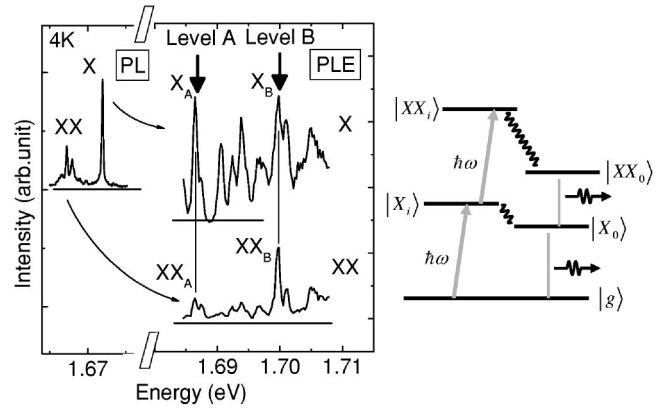


FIG. 1. PL and broadband PLE spectra of the exciton (X) and biexciton (XX). The excitation intensity is about 250 W/cm^2 . The energy level structures for levels A and B are shown in right hand side. The suffix “i” represents “A” or “B.”

vapor phase epitaxy (MOVPE). Our quantum dot is a self-assembled quantum dot and we call this quantum dot a quantum disk because of its shape. The quantum disk has a unique feature in that the lateral size is tunable by controlling the growth conditions. Moreover, the quantum disk has no wetting layers, which are usually present in other self-assembled quantum dots grown in the Stranski-Krastanov mode. The fabrication process has already been reported in detail.^{21,22} Measurements were performed using the micro-PL method. The excitation laser light from a cw wavelength tunable Ti-sapphire laser was focused on the quantum dot sample with a microscope objective lens (spot size $2 \mu\text{m}$) through a metal mask with holes processed on the sample surface (hole size $0.5 \mu\text{m}$). The sample was mounted on the cold head in a liquid He cooled cryostat. The PL was collected by the lens and detected by a liquid nitrogen cooled charge coupled device through a high-resolution spectrometer. This method enables us to measure the PL properties from a single dot. PL measurement with the scanning wavelength of the excitation laser gives PL excitation (PLE) spectra that directly reflect the photoabsorption spectra and energy structure of the quantum dot. We evaluated the coherent effects from the PL and photoabsorption spectra in a single InGaAs quantum dot.

III. RESULTS AND DISCUSSION

Figure 1 shows an example of the PL and PLE in a quantum dot recorded at 4 K. The excitation density estimated is 250 W/cm^2 . The indium content of the quantum dot is about 0.4. The average lateral size and thickness are 30 nm and 3 nm, respectively. Exciton related PL and other PL peaks are observed separately. We employed a previously reported method to confirm the biexciton PL emission.¹⁴ The method uses the power dependence of the PL intensity at a relatively low excitation power and the peak structure of the PLE spectrum to assign PL emissions. We concluded that the PL emission is for the biexciton when the PL intensity is quadratically dependent on the excitation power and when the PL has a similar PLE spectrum to that of the exciton. The PL peak

denoted as the biexciton in Fig. 1 meets both conditions. We focus these exciton- and biexciton-related PL peaks. The energy separation between the exciton and biexciton PL corresponds to the biexciton binding energy. The other PL peak may originate from a charged exciton.^{23,24}

PL measurements undertaken using scanning excitation laser energy provide us with PLE spectra. Since the PLE spectra were obtained from the PL signals from a single quantum dot, the spectra are completely free from any inhomogeneous broadening effects. The PLE in the single quantum dot has a unique feature whereby the exciton and biexciton absorption spectra can be selectively obtained simply by changing the PL detection energy. The PLEs are also shown in Fig. 1. These correspond to the absorption spectra for an exciton (X) and a biexciton (XX) in a single quantum dot. Many discrete peaks can be seen in Fig. 1. Each PLE peak exhibits a higher state for an exciton or a biexciton. These discrete peaks are characteristic of a zero-dimensional structure. In this study, we focus on two higher states denoted as levels A and B. In these levels, large signals can be seen in exciton (X_A and X_B) as well as biexciton absorption (XX_A and XX_B). Figure 1 also shows the simplified energy level structure for these levels. When the laser light is set at these energies, an exciton and a biexciton states are simultaneously populated by the excitation laser. These populations relax to their lowest states X_0 and XX_0 leading to exciton and biexciton PL emissions. The PLE signal of XX_A is smaller than that of XX_B in Fig. 1. This is because the optical dipole moment between XX_A and X_A is smaller than that between XX_B and X_B . However, the energy structure itself for these states is the same coherently coupled five level system. We evaluate the coherent effects between an exciton and a biexciton using these levels. The energy difference between the PL detection energy and X_A is about 30 meV. This difference is close to the LO phonon energy. However, the contribution of the LO phonon to the PL emission is negligible because the photoemission efficiency of our quantum dot is of the same order as that for usual quantum wells. Moreover, no replica structure can be seen in the PLE spectra.

In the system shown in Fig. 1, optical dipoles are excited between X_i and g , and between XX_i and X_i ($i=A$ or B). Both these dipoles include the X_i state. Therefore, exciton coherence and its absorption spectrum should include the effects of biexciton-related coherence. Additionally, an exciton is composed of an electron and a hole. A biexciton is a combined state of two excitons. Their populations increase linearly with excitation intensity and with the square of the intensity, respectively. This means that the ratio of the exciton to biexciton populations changes with intensity. Therefore, the intensity dependence of the exciton absorption gives us information on biexciton effects. Moreover, optical dipole moment dependence can be discussed by comparing the intensity dependence of levels A and B.

The populations of the X_i and XX_i states are created by coherent interactions in this XX_i - X_i - g system as shown in Fig. 1. These populations each relax into their lowest states (X_0 and XX_0) through incoherent processes such as acoustic phonon emission processes. The populations of X_0 and XX_0 are linearly dependent on the populations of the X_i and XX_i

states. The X_0 and XX_0 states emit PL signals whose intensities are proportional to the populations of the X_0 and XX_0 states. Thus, the coherent effects in the X_i and XX_i states are directly reflected in the PL signals. Note that the coherent effects occur only in the XX_i - X_i - g system and the relaxation processes into each lowest state are incoherent processes. Therefore, our system is substantially a coherent three-level system and the other two levels act as states for the observation of the coherent effects. Thus, the coherent effects are evaluated from the PL and PLE measurements.

Figure 2 shows the exciton and biexciton absorption spectra for three excitation power densities. The power dependence of the absorption spectra in level A is completely different from that in level B. In level A, the absorption spectra for X_A and XX_A both exhibit Lorentzian shapes against excitation power. Absorption linewidths increase with excitation intensity, which are caused by the power broadening effects. This effect is more prominent in the X_A state than in the XX_A state. Coherent coupling effects between the X_A and XX_A states induce larger broadening in the X_A state.¹⁶ In contrast, the spectral shapes of the absorption spectra in level B vary greatly with excitation intensity. The absorption spectra in X_B and XX_B have Lorentzian shapes for 250 W/cm² similar to those for level A. With increasing excitation power density, the XX_B absorption spectra exhibit the power broadening effect. This dependence is similar to that in level A. However, the dependence of X_B absorption is completely different from this. The X_B absorption spectrum changes from a Lorentzian shape to an unusual shape with a dip-shaped structure centered on the exciton resonant energy, which is the peak energy for 250 W/cm². These unusual line shapes have not yet been clearly observed in other systems such as bulk and quantum wells. We consider these unusual spectra to be caused by strong coherent coupling effects between the X_B and XX_B states.

Coherent coupling effects should depend strongly on excitation intensity. Previously, Rabi oscillations were observed in the quantum dots and the Rabi frequencies and corresponding Rabi splitting energies increased with the square root of the excitation.²⁵⁻²⁷ The dip-shaped spectra in X_B can be regarded as absorption spectra with two split states. When the dip-shaped spectra are caused by coherent effects, the intensity dependence of the energy splitting may provide insights into the origins of the dip-shaped spectra. Figure 3 plots the energy splitting as a function of excitation intensity. A square root function and a linear function are shown for a comparison. These plots fit the square root function rather than the linear function. This dependence is the same as that of the Rabi splitting in two-level systems. In the XX_B - X_B - g system, all three levels are coherently coupled. However, when the dipole moment between X_B and XX_B is much larger than that between g and X_B , this system behaves like a two-level XX_B - X_B system probed by X_B - g . This two-level system might induce Rabi splitting where the energy splitting has a square root dependence of excitation intensity as shown in Fig. 3. The square root dependence indicates that the dip-shaped spectra are caused by strong coherent effects in the XX_B - X_B states.

In the coherently coupled XX_B - X_B - g system, the coherent effects should be strongly influenced by the population of

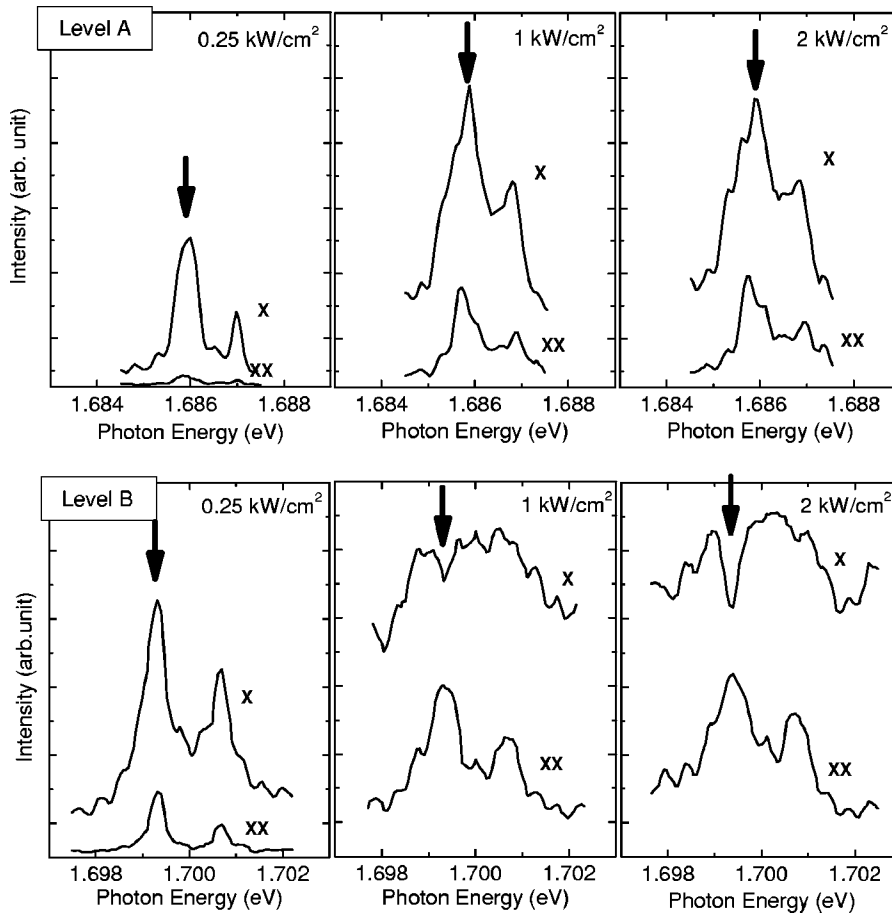


FIG. 2. PLE spectra of X and XX for three excitation powers for levels A and B. In the results for level B, the PLE spectrum of X changes from a Lorentzian-shaped to a dip-shaped structure with increasing excitation. All spectra are obtained with high energy resolution compared with the results in Fig. 1.

each state. We consider the XX_B-X_B-g system for excitation lights with different polarizations. The energy level structure for XX_B-X_B-g is rewritten in Fig. 4(a) for an excitation light with a linear polarization. A linearly polarized light is a linear combination of circularly polarized lights and can create an all states population as $X_B\uparrow$, $X_B\downarrow$, and XX_B . In contrast, using circularly polarized excitation light may suppress the transition of XX_B-X_B reflecting a selection rule in the Bloch functions of the XX_B states.¹²⁻¹⁴ For example, an excitation light with a counterclockwise polarization only creates the

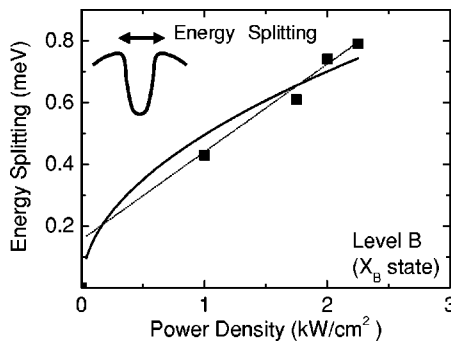


FIG. 3. Power dependence of dip-shaped structure shown in Fig. 2. The energy splitting is the width of the dip-shaped structure. The solid line shows a fitted curve which is proportional to a square root of the power density. The dotted curve is linear dependence for a comparison. The inset shows a schematic dip-shaped spectrum and energy splitting.

$X_B\uparrow$ state as in Fig. 4(b). This system is just a two-level system of $X_B\uparrow-g$ and none of the coherent effects in XX_B-X_B may appear in the absorption spectra of X_B-g . Figure 4 shows exciton PL and absorption spectra for linearly and circularly polarized excitation lights. The excitation intensities are 2 kW/cm^2 . For linearly polarized excitation, the exciton absorption spectrum shows a dip-shaped spectrum for an intense linearly polarized light. Whereas for circularly polarized excitation, the exciton absorption spectrum exhibits a broadened Lorentzian shape. The biexciton absorption spectrum is much smaller than that for linearly polarized excitation. This means that the circularly polarized excitation light cannot efficiently create a biexciton. This small population of the biexciton state leads to negligible coherent effects in the XX_B-X_B states. The absorption properties are determined solely by the X_B-g transition resulting in a broadened Lorentzian absorption spectrum with no coherent features. Figure 4 provides proof that coupling effects in the XX_B-X_B states yield dip-shaped spectra. Moreover, we found that the coherent effects of XX_B can be controlled by using optical selection rules for the X_B-g and XX_B-X_B transitions with polarization of excitation lights.

In strongly excited bulk and quantum wells, interactions among many excitons lead to changes in the absorption spectra (exciton many body effects).²⁸ In the quantum dot, we can accurately estimate the number of excitons from the PL emission energy; the single exciton emission process can be distinguished from the two exciton-related emission process (relaxation from a biexciton to an exciton). The two exciton-

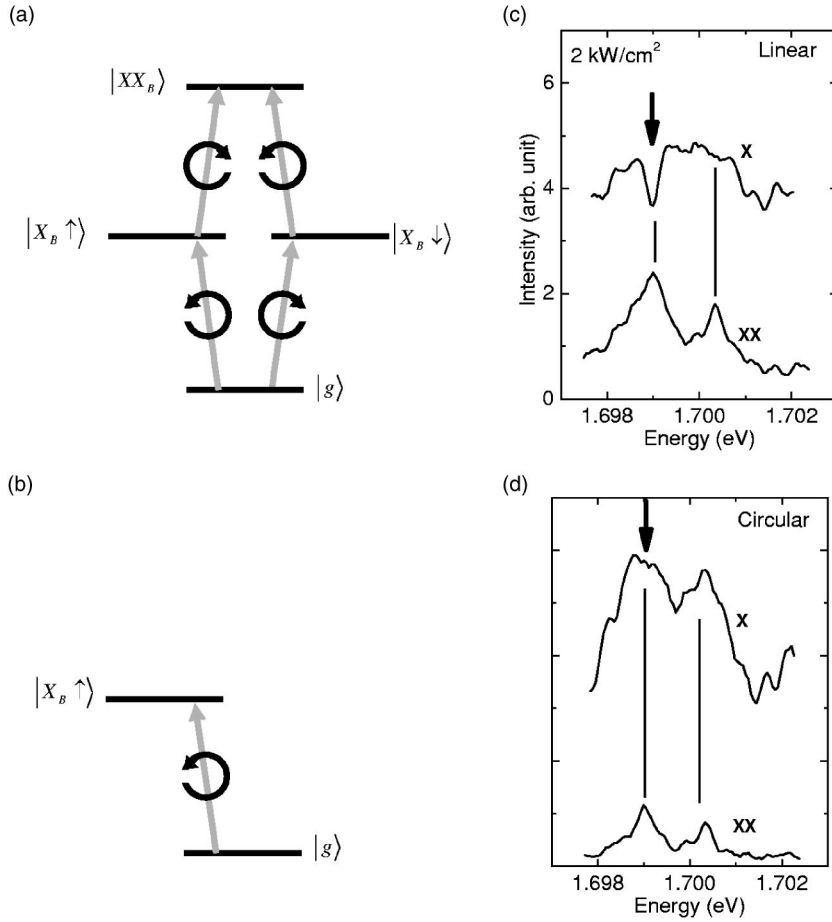


FIG. 4. Energy level structures in the XX_B - X_B - g system for a linearly polarized excitation light (a) and a circularly polarized light (b). PLE spectra for a linearly polarized excitation light (c) and a circularly polarized light (d). The linearly polarized light, which is expressed as a linear combination of two opposite circularly polarized lights, can create the X_B states of spin-up ($X_B\uparrow$) and spin down ($X_B\downarrow$).

related emission process involves a kind of many body effect with two excitons. When we measure exciton-related PL and PLE spectra, they reflect single exciton properties regardless of excitation power. According to the exciton many body effects, the lineshapes of PL and PLE spectra measured by single exciton PL are independent of excitation power and the number of excitons created by the excitation light.

Conventional theoretical analyses of many body effects are based on a many body Hamiltonian that includes the Coulomb interaction between two particles (electron-electron, hole-hole, and electron-hole). An analysis of biexciton properties requires a Coulomb interaction between four particles (two electrons and two holes) and this has not yet been reported. Moreover, no theory deals with the coupling effects between an exciton and a biexciton. As an origin for the measurement results, we considered coherent coupling effects with exciton and biexciton states and quantum interference effects. Since no microscopic theory has yet been reported to verify these effects, we analyze the exciton-biexciton system with a simple theory and simulate the main features of the experimental results.

The exciton-biexciton system can be regarded as a five-level system shown as Fig. 5. In the measurements, we detected exciton and biexciton PL signals from X_0 and XX_0 , respectively. We use a density-matrix method to analyze the optical responses in this five-level system interacting with an excitation light.²⁹ Dipole transitions are considered in the X_i - g and XX_i - X_i states. The dimensions of the density matrix

ρ are 5×5 . When the nondiagonal elements in ρ are not zero, coherent effects exist in corresponding states. We disregard the coherent effects in the X_i - X_0 and XX_i - XX_0 transitions because these transition energies are largely nonresonant to the excitation light; coherent effects occur only in the XX_i - X_i - g states. The system may be analyzed by using the following equations:

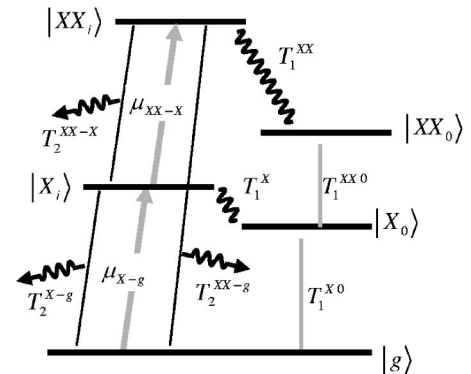


FIG. 5. Energy level structure and physical parameters used in the theoretical analysis. Coherent effects are included only in XX_i - X_i and X_i - g with dipole moments of μ_{XX-X} and μ_{X-g} . The relaxation processes from XX_i and X_i to XX_0 and X_0 are incoherent processes characterized by T_1^{XX} and T_1^X . The PL signals correspond to relaxations in XX_0 - X_0 with T_1^{XX0} and X_0 - g with T_1^{X0} for biexciton and exciton PLs, respectively.

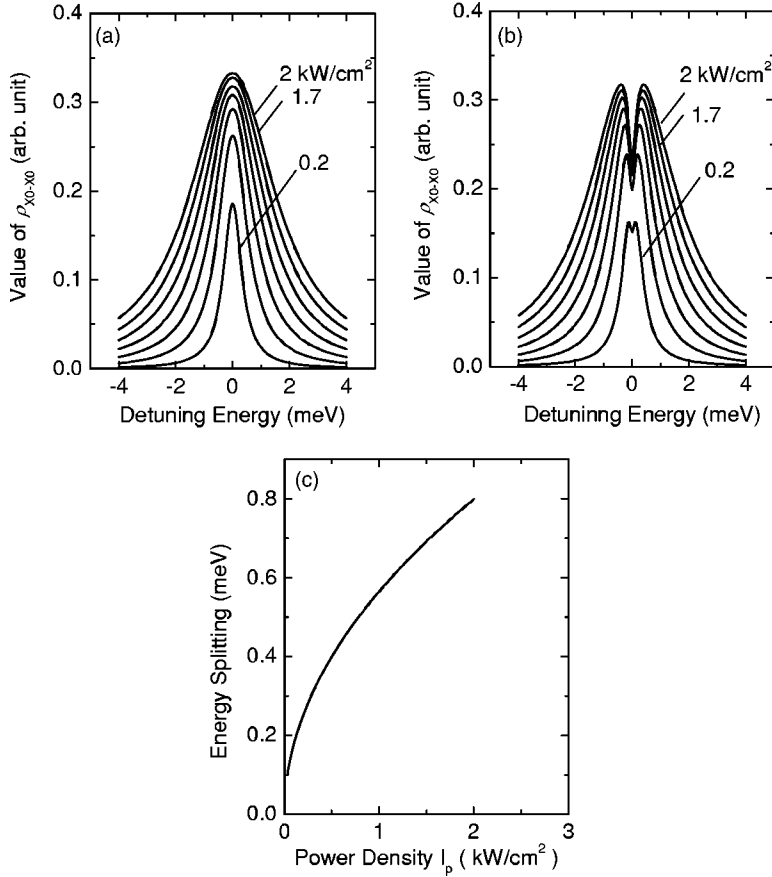


FIG. 6. Exciton population ρ_{X0-X0} as a function of detuning energy for different excitation powers and different μ_{XX-X} . (a) $\mu_{XX-X} = \mu_{X-g}$ and (b) $\mu_{XX-X} = 20\mu_{X-g}$. The ρ_{X0-X0} plots from 0.2 to 2 kW/cm² in 0.3 kW/cm² steps. The detuning energy of zero is for an excitation light with resonant energy to exciton energy. (c) The energy splitting in (b) as a function of power density.

$$\dot{\rho}_{g-g} = -i\Omega_{X-g}(d_{X-g}^* - d_{X-g}) + \Gamma_{X0}\rho_{X0-X0}, \quad (1)$$

$$\begin{aligned} \dot{d}_{X-g} = & -i\Delta_{X-g}d_{X-g} + i\Omega_{X-g}(\rho_{g-g} - \rho_{X-X}) + i\Omega_{XX-X}d_{XX-g} \\ & - \gamma_{X-g}d_{X-g}, \end{aligned} \quad (2)$$

$$\dot{\rho}_{X-X} = i\Omega_{X-g}(d_{X-g}^* - d_{X-g}) - i\Omega_{XX-X}(d_{XX-X}^* - d_{XX-X}) - \Gamma_X\rho_{X-X}, \quad (3)$$

$$\begin{aligned} \dot{d}_{XX-g} = & -i\Delta_{XX-g}d_{XX-g} + i\Omega_{XX-X}d_{X-g} - i\Omega_{X-g}d_{XX-X} \\ & - \gamma_{XX-g}d_{XX-g}, \end{aligned} \quad (4)$$

$$\begin{aligned} \dot{d}_{XX-X} = & -i\Delta_{XX-X}d_{XX-X} + i\Omega_{XX-X}(\rho_{X-X} - \rho_{XX-XX}) \\ & - i\Omega_{X-g}d_{XX-g} - \gamma_{XX-X}d_{XX-X}, \end{aligned} \quad (5)$$

$$\dot{\rho}_{X0-X0} = \Gamma_X\rho_{X-X} + \Gamma_{XX0}\rho_{XX0-XX0} - \Gamma_{X0}\rho_{X0-X0}, \quad (6)$$

$$\dot{\rho}_{XX0-XX0} = \Gamma_{XX}\rho_{XX-XX} - \Gamma_{XX0}\rho_{XX0-XX0}, \quad (7)$$

$$\rho_{g-g} + \rho_{X-X} + \rho_{XX-XX} + \rho_{X0-X0} + \rho_{XX0-XX0} = 1, \quad (8)$$

where $\Gamma = 1/T_1$, $\gamma = 1/T_2$, and $\Omega = \mu E / 2\hbar$. The constants T_1 , T_2 , μ , and E are the population relaxation time, the dephasing time, the dipole moment, and the electric field of the light, respectively. The detuning energy $\hbar\Delta_i$ is defined as $\hbar\Delta_i = E_i - E_{ph}$, where E_i is the transition energy between two states and E_{ph} is the photon energy of the excitation light. Zero

biexciton binding energy is assumed from the experimental results in Fig. 1. This means that $\Delta_{X-g} = \Delta_{XX-X} = \Delta_{XX-g}/2$. Numerical calculations for steady states for excitons yield exciton PLE spectra as ρ_{X0-X0} . The calculations also yield results on biexcitons as $\rho_{XX0-XX0}$. We first consider ρ_{X0-X0} for exciton and discuss the results on biexcitons later.

Figures 6(a) and 6(b) show ρ_{X0-X0} as a function of detuning energy for different powers. The energy zero is for the resonant light energy with the exciton resonance. In this calculation, we used numerical constants; certain parameters such as Γ_{X0} and Γ_{XX0} were determined taking our other measurement results into consideration.³⁰ Other parameters were chosen so that the calculated results fitted the experimental results. Specific values are as follows: $T_1^X = 100$ ps, $T_1^{XX} = 50$ ps, $T_1^{X0} = 500$ ps, $T_1^{XX0} = 500$ ps, $T_2^{X-g} = 2$ ps (0.2 kW/cm²), $T_2^{X-g} = 0.5$ ps (2 kW/cm²), $T_2^{XX-X} = 2$ ps (0.2 kW/cm²), $T_2^{XX-X} = 1.5$ ps (2 kW/cm²), $T_2^{XX-X} = 3$ ps and μ_{X-g} of the dipole moment of GaAs bulk. Intensity dependent dephasing times are included as each γ changes linearly with excitation power from 0.2 to 2 kW/cm². The theoretical analyses considered the intensity dependent effects and predicted novel phenomena such as controllable Rabi oscillations.³¹⁻³³ Figures 6(a) and 6(b) are for different μ_{XX-X} ; $\mu_{XX-X} = \mu_{X-g}$ for (a) and $\mu_{XX-X} = 20\mu_{X-g}$ for (b).

In Fig. 6(a), the linewidths of ρ_{X0-X0} broaden with increasing excitation; however, the line shapes have Lorentzian-type peak shapes. Whereas in Fig. 6(b), the line shapes are almost Lorentzian-type for weak excitations and

those change into a dip-shaped spectrum with increasing intensity. The calculated results in Figs. 6(a) and 6(b) are similar to the measured results for levels A and B, respectively. Figure 6(b) was calculated using a larger dipole moment μ_{XX-X} than that in Fig. 6(a). The dipole moment directly characterizes the strength of the coherence between XX and X; a larger μ_{XX-X} causes larger coherent effects. Therefore, we attribute the dip-shaped exciton absorption spectra to strong coherent coupling between the exciton and biexciton states. Figure 6(c) shows the widths of the dip as a function of excitation intensity. The intensity dependence shows the square root dependence of excitation intensities. This dependence is the same as seen in the experimental results in Fig. 3. Moreover, this result ensures that the dip-shaped absorption spectra can be interpreted in terms of Rabi splitting between an exciton and a biexciton state. Our simple theoretical analysis simulated the main features of the experimental results. The experimental results can be interpreted in terms of coherent effects between an exciton and a biexciton state.

Our simple theory has only three levels for analyzing the coherent effects. Actual quantum dots may exhibit the effects of other exciton states and interactions among many excitons. These effects might modify our interpretation especially as regards the biexciton absorption properties. However, these effects are nonresonant effects for the exciton state we focused on. The main interaction relevant to the dip shaped interaction is an energetically resonant interaction between the exciton and biexciton states.

Our theory can be applied to interpret absorption properties in excitons. However, our theory is not particularly valid for analyzing biexciton properties. Biexcitons can be created through different exciton states, which are not covered by the theory. When the exciton absorption becomes small due to coherent interactions, such effects may determine the biexciton absorption properties. These effects are very important in terms of the detailed microscopic theory of exciton systems in quantum dots. This subject may be considered in future work.

We discuss the dip-shaped absorption spectra using the dressed state model. With a weak excitation, the energy level structure is a usual three level system and the absorption spectra for both the exciton and biexciton have Lorentzian shapes. With a strong excitation, the exciton and biexciton states couple strongly and form dressed states with energy splitting that depend on the Rabi frequency. This causes the absorption to disappear at the exciton resonant energy and this results in an absorption spectrum with a dip-shaped structure. The dressed state model explains our measurement and calculation results intuitively.

This effect can also be interpreted as a quantum interference effect mediated by exciton and biexciton absorptions. This system is simply a three-level cascade-type electromagnetically induced transparency (EIT).^{17,18} In our system, there are at least two possible paths for excitonic absorption; a direct optical transition in X-g and an optical transition via the XX state (X-XX-X-g). The phase of the latter transition is opposite to that of the former. Therefore, destructive interference mediated by these two transitions makes the net optical absorptions in X-g disappear. This result is just EIT. Our results indicate that novel optical device functions pre-

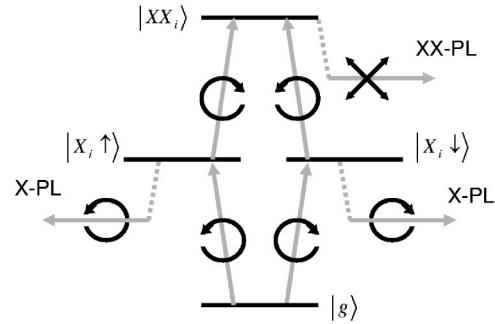


FIG. 7. Energy diagram for accessing and observing four distinguishable states. Circularly polarized light can distinctively create $X_i \uparrow$ or $X_i \downarrow$ excitons. These excitons emit PL whose polarizations are the same as the excitation. Linearly polarized light can excite a XX_i biexciton. The biexciton emits PL whose energy is lower than the exciton PL by the biexciton binding energy.

dicted with EIT such as coherent trapping, slowing light and inversion-less laser emission may be demonstrated in quantum dots.

Our experimental and theoretical results clearly showed that coherent effects in an exciton and a biexciton states occur in a quantum dot and that these effects can be controlled by controlling the polarization of the excitation light. We propose a scheme for accessing four distinguishable states based on our results. Figure 7 shows our scheme schematically. Four states (g , $X_i \uparrow$, $X_i \downarrow$, and XX_i) are shown in Fig. 7. We assume that the biexciton energy is twice the exciton energy. By illuminating circularly polarized excitation light, we can create $X \uparrow$ or $X \downarrow$, and we can select two states in terms of polarization direction. A linearly polarized excitation light can create the XX_i state. Each of the four states can be observed by detecting the PL: g , $X_i \uparrow$, $X_i \downarrow$, and XX_i emit no PL, circularly polarized X-PL (counterclockwise direction), circularly polarized X-PL (clockwise direction) and XX-PL, respectively. Each PL is easily distinguished from the others by using bandpass filters and polarization optics. This scheme could be applied to a two-bit quantum gate such as controlled NOT with an exciton-biexciton system and an excitation light for gate control. The characteristic of the scheme is the use of an excitation light to access four states. Since the exciton energy is assumed to be the same as the biexciton energy, the control lights for the four states can be supplied from a single laser source. Different states can be controlled by using polarization optics. When the exciton energy is different from the biexciton energy, a phase lock technique is required for two light sources with different energies, and this is not easy to realize with conventional laser sources. Moreover, the required laser power is not very large even for the large nonlinear optical processes in the exciton-biexciton system. An excitation light whose intensity is several photons is sufficient to control this system because a single photon can excite an exciton and one more photon can excite a biexciton. The optical nonlinearity effects require just a single excitation light whose intensity is as weak as the several photon region and which is supplied by a single light source. Our scheme offers a major advantage with respect to demonstrating quantum gate operation with two Q-bits.

The exciton-biexciton optical nonlinearity relies on a larger dipole moment in a biexciton than that in an exciton. Here, we consider the reason for this larger dipole moment. The biexciton is composed of two excitons with negligible binding energy as shown in Fig. 1. This biexciton can be regarded as two weakly correlated excitons confined in a quantum dot potential and even as two independent excitons. The transition probability between the two independent excitons and the single exciton will be twice that between the single exciton and the ground state. A theoretical analysis, which calculates the dipole moment of biexcitons, supports our view.¹² In this calculation, the dipole moment of two weakly correlated excitons becomes twice that of an independent single exciton in a relatively strong confinement regime. The dipole moment may be larger in a mesoscopic confinement regime such as our quantum dots by analogy with the mesoscopic enhancement of the dipole moment in a single exciton. These weakly correlated excitons may lead to the strong coherence and the dip-shaped absorption spectra. Moreover, our result may reflect a kind of Bosonic feature of excitons. Bosonic particles can exist at the same energy, and the dipole moment of bosons increases linearly with the number of particles. A huge dipole moment may appear in many excitons. The interpretation of our results almost meets these conditions. Confirmation of this interpretation requires further experimental and theoretical studies. These studies would provide new perspective on the exciton physics of quantum dots.

IV. CONCLUSION

We investigated the coherent coupling effects in an exciton and a biexciton in a single quantum dot. We measured the absorption properties in an InGaAs quantum dot by employing the micro-PL method and the excitation intensity dependence of exciton and biexciton absorptions for two exciton higher states. The power dependence shows a distinct

contrast in the two exciton states. In the exciton state of the more efficient biexciton creation, there are unusual absorption line shapes with a dip-shaped structure in the high excitation condition. This dip width energy has a square root dependence with increasing excitation intensity. This result indicates that the dip-shaped structure was caused by the Rabi oscillation, which is well-known as a coherent effect in coupled electron-photon systems. The dip-shaped structure appeared only with a large biexciton state population. The use of circularly polarized light suppressed the biexciton population and yielded only the usual Lorentzian-type line shape. All our experimental results can be interpreted in terms of strong coherent coupling effects between exciton and biexciton states. A theoretical analysis using a five-level density matrix simulated the main features of the experimental results. We qualitatively explained our results using the dressed state model.

Our results reveal that strong coherent effects are achieved in a quantum dot due to coupling between an exciton and a biexciton. Moreover, these are also interpreted as a cascade-type EIT in an exciton-biexciton system. These coherent effects can be controlled by using the polarization direction of the excitation light. This provides us with a scheme for accessing four distinguishable states, which may be applied to a demonstration of quantum gate operation with two Q-bits. These results give novel exciton physics in quantum dots and make an important contribution to the realization of quantum devices with quantum dots.

ACKNOWLEDGMENTS

We express our sincere thanks to Dr. Y. Hirayama for encouragement throughout this work. We also thank Drs. H. Nakano, T. Sogawa, M. Kumagai, and T. Tawara for fruitful discussions on exciton optical properties of semiconductors. Part of this work was supported by the National Institute of Information and Communications Technology (NICT).

*Present address: Faculty of Engineering, Kansai University, 3-3-35, Yamate-cho, Suita-shi, Osaka 564-8680, Japan

¹Y. Arakawa and H. Sakaki, *Appl. Phys. Lett.* **40**, 939 (1982).

²D. Bimberg, N. Kirxtaedler, N. N. Ledentsov, Zh. I. Alferov, P. S. Kopev, and V. M. Ustinov, *IEEE J. Quantum Electron.* **3**, 196 (1997).

³D. P. Divincenzo, *Science* **270**, 255 (1995).

⁴E. Waks, K. Inoue, C. Santori, D. Fattal, J. Vuckovic, G. Solomon, and Y. Yamamoto, *Nature (London)* **420**, 762 (2002), and references therein.

⁵M. Bayer, P. Hawrylak, K. Hinzer, S. Fafard, M. Korkusinski, Z. R. Wasilewski, O. Stern, and A. Forchel, *Science* **291**, 451 (2001).

⁶T. H. Stievater, X. Li, D. G. Steel, D. Gammon, D. S. Katzer, D. Park, C. Piermarocchi, and L. J. Sham, *Phys. Rev. Lett.* **87**, 133603 (2001).

⁷H. Kamada, H. Gotoh, J. Temmyo, T. Takagahara, and H. Ando, *Phys. Rev. Lett.* **87**, 246401 (2001).

⁸H. Htoon, T. Takagahara, D. Kulik, O. Baklenov, A. L. Holmes, Jr., and C. K. Shih, *Phys. Rev. Lett.* **88**, 087401 (2001).

⁹P. Borri, W. Langbein, S. Schneider, U. Woggon, R. L. Sellin, D. Ouyang, and D. Bimberg, *Phys. Rev. Lett.* **87**, 157401 (2001).

¹⁰D. Birkedal, K. Leosson, and J. M. Hvam, *Phys. Rev. Lett.* **87**, 227401 (2001).

¹¹M. Bayer and A. Forchel, *Phys. Rev. B* **65**, 041308(R) (2002).

¹²S. V. Nair and T. Takagahara, *Phys. Rev. B* **55**, 5153 (1997).

¹³M. Bayer, S. N. Walck, T. L. Reinecke, and A. Forchel, *Phys. Rev. B* **57**, 6584 (1998).

¹⁴H. Kamada, H. Ando, J. Temmyo, and T. Tamamura, *Phys. Rev. B* **58**, 16243 (1998).

¹⁵X. Li, Y. Wu, D. Steel, D. Gammon, T. H. Stievater, D. S. Katzer, D. Park, C. Piermarocchi, and L. J. Sham, *Science* **301**, 809 (2003).

¹⁶H. Gotoh, H. Kamada, T. Saitoh, H. Ando, and J. Temmyo, *Phys. Rev. B* **69**, 155328 (2004).

¹⁷S. E. Harris, J. E. Field, and A. Imamoglu, *Phys. Rev. Lett.* **64**,

- 1107 (1990).
- ¹⁸M. O. Scully and M. S. Zubairy, *Quantum Optics* (Cambridge University Press, Cambridge, 1997).
- ¹⁹T. Takagahara and E. Hanamura, *Phys. Rev. Lett.* **56**, 2533 (1986).
- ²⁰E. Hanamura, *Phys. Rev. B* **38**, 1228 (1988).
- ²¹R. Nötzel, J. Temmyo, and T. Tamamura, *Nature (London)* **369**, 131 (1994).
- ²²J. Temmyo, R. Nötzel, and T. Tamamura, *Appl. Phys. Lett.* **71**, 1086 (1997).
- ²³J. G. Tischler, A. S. Bracker, D. Gammon, and D. Park, *Phys. Rev. B* **66**, 081310(R) (2002).
- ²⁴L. Besombes, J. J. Baumberg, and J. Motohisa, *Phys. Rev. Lett.* **90**, 257402 (2003).
- ²⁵K. Brunner, G. Abstreiter, G. Böhm, G. Tränkle, and G. Weimann, *Phys. Rev. Lett.* **73**, 1138 (1994).
- ²⁶H. Kamada, H. Gotoh, H. Ando, J. Temmyo, and T. Tamamura, *Phys. Rev. B* **60**, 5791 (1999).
- ²⁷G. Chen, T. H. Stievater, E. T. Batteh, X. Li, D. G. Steel, D. Gammon, D. S. Katzer, D. Park, and L. J. Sham, *Phys. Rev. Lett.* **88**, 117901 (2002).
- ²⁸S. Koch, *Quantum Theory of the Optical and Electronic Properties of Semiconductors* (World Scientific, Singapore, 1990).
- ²⁹For example, M. D. Levenson and S. S. Kano, *Introduction to Nonlinear Laser Spectroscopy* (Academic, Orlando, 1988).
- ³⁰H. Gotoh, H. Kamada, H. Ando, and J. Temmyo, *Jpn. J. Appl. Phys., Part 1* **42**, 3340 (2003).
- ³¹J. Förstner, C. Weber, J. Danckwerts, and A. Knorr, *Phys. Status Solidi B* **238**, 419 (2003).
- ³²J. Förstner, C. Weber, J. Danckwerts, and A. Knorr, *Phys. Rev. Lett.* **91**, 127401 (2003).
- ³³U. Hohenester and G. Stadler, *Phys. Rev. Lett.* **92**, 196801 (2004).